	Form Approved OMB NO. 0704-0188

1. AGENCY USE ONLY (Leave Blank)	2. REPORT DATE	3. REPORT TYPE AND DATES COVERED
	May 26th, 2008	Final report

4. TITLE AND SUBTITLE	5. FUNDING NUMBERS
Multi-scale modeling of proton transport, water distribution, and methanol permeability in Proton Exchange Membranes (PEMs)	W911NF-07-1-0085
6. AUTHOR(S) Stephen J. Paddison, PI & Mark E. Tuckerman, co-PI	
7. PERFORMING ORGANIZATION NAME(S) AND ADDRESS(ES) University of Alabama in Huntsville New York University	8. PERFORMING ORGANIZATION REPORT NUMBER
9. SPONSORING / MONITORING AGENCY NAME(S) AND ADDRESS(ES) U. S. Army Research Office P.O. Box 12211 Research Triangle Park, NC 27709-2211	10. SPONSORING / MONITORING AGENCY REPORT NUMBER 50629.1-CH

11. SUPPLEMENTARY NOTES

The views, opinions and/or findings contained in this report are those of the author(s) and should not be construed as an official Department of the Army position, policy or decision, unless so designated by other documentation.

12 a. DISTRIBUTION / AVAILABILITY STATEMENT	12 b. DISTRIBUTION CODE
Approved for public release; distribution unlimited.	

13. ABSTRACT (Maximum 200 words)

We undertook a multiscale modeling of proton exchange membranes through three simultaneous but distinct studies of perfluorosulfonic acid (PFSA) systems at different time and length scales: (1) hydrated morphology of PFSA membranes with dissipative particle dynamics (DPD) simulations; (2) classical MD simulations of the hydration and hydronium ion diffusion of the short-side chain (SSC) PFSA membrane; and (3) ab initio density functional theory Car-Parrinello MD simulations of model PFSA systems. A course-grained study of the hydrated morphology of Nafion and the SSC ionomer as a function of water content and equivalent weight (EW) was undertaken using DPD simulations. The results were analyzed through water contour plots, radial distribution functions of the water, and scattering plots. This work provides an insight into how ionomer EW and side chain chemistry effect morphology. In the second study a unique force field was derived for the fully atomistic MD simulations of the SSC ionomer. The EW was fixed but the water content (from minimal to intermediate) was varied. Structural data and proton diffusion coefficients were computed on a small system of the SSC ionomer and provide a base line for simulations that treat the atoms as classical particles only. Finally, we performed density functional theory Car-Parrinello MD simulations of the mono-, di- and tetra- hydrates of trifluoromethanesulfonic acid as model systems for minimally hydrated PFSA polymers. We developed a consistent set of dispersion corrected atom-centered potentials to account for van der Waals interactions in these solids in order to match structural and lattice parameters

14. SUBJECT TERMS	15. NUMBER OF PAGES
	16. PRICE CODE

17. SECURITY CLASSIFICATION OR REPORT	18. SECURITY CLASSIFICATION ON THIS PAGE	19. SECURITY CLASSIFICATION OF ABSTRACT	20. LIMITATION OF ABSTRACT
UNCLASSIFIED	**UNCLASSIFIED**	**UNCLASSIFIED**	**UU**

FINAL PROGRESS REPORT

For Grant # W911NF-07-1-0085

Multi-scale modeling of proton transport, water distribution, and methanol permeability in Proton Exchange Membranes (PEMs)

(1) Foreword

We have undertaken our multiscale modeling of proton exchange membranes through three simultaneous but distinct studies of perfluorosulfonic acid (PFSA) systems at different time and length scales: (1) hydrated morphology of PFSA membranes with dissipative particle dynamics (DPD) simulations; (2) classical MD simulations of the hydration and hydronium ion diffusion of the short-side chain (SSC) PFSA membrane; and (3) *ab initio* density functional theory Car-Parrinello MD simulations of model PFSA systems. A course-grained study of the hydrated morphology of Nafion and the SSC ionomer as a function of water content and equivalent weight (EW) was undertaken using DPD simulations. The results were analyzed through water contour plots, radial distribution functions of the water, and scattering plots. This work provides the first insight into how EW and side chain chemistry of the ionomer effects morphology. In the second study a unique force field was derived for the fully atomistic MD simulations of the SSC ionomer. The EW was fixed but the water content (from minimal to intermediate) was varied. Structural data and proton diffusion coefficients were computed on a small system of the SSC ionomer and provide a base line for simulations that treat the atoms as classical particles only. Finally, we performed density functional theory Car-Parrinello MD simulations of the mono-, di- and tetra- hydrates of trifluoromethanesulfonic acid as model systems for minimally hydrated PFSA polymers. We developed a consistent set of dispersion corrected atom-centered potentials to account for van der Waals interactions in these solids in order to match structural and lattice parameters.

(2) Table of Contents

Report is less than 10 pages so omitted.

(3) List of Appendixes, Illustrations and Tables

Nothing to append. No Tables.

Figure 1. Morphologies of the SSC and Nafion PFSA membranes at a hydration level where $\lambda = 9$.
Figure 2. Morphologies of the SSC and Nafion PFSA membranes at a hydration level where $\lambda = 16$.
Figure 3. Radial distribution functions, G(*r*)'s, of water particles at three distinct water contents.
Figure 4. An ion cage exhibiting very short S–S distances in the MD simulation of the SSC ionomer.
Figure 5: Snapshots of the (a) $H_3O^+CF_3SO_3^-$, (b) $H_5O_2^+CF_3SO_3^-$, and (c) $H_9O_4^+CF_3SO_3^-$ systems.
Figure 6. Snapshot of proton defects in the $H_3O^+CF_3SO_3^-$ system found in (a) this study and (b) by Eikerling *et al.*
Figure 7. (a) Close-up of a proton defect and its (b) location, highlighted by the box, within the defective $H_5O_2^+CF_3SO_3^-$ crystal.
Figure 8. Snapshot of a Grotthuss-type proton transfer event in $H_9O_4^+CF_3SO_3^-$.

(4) Statement of the problem studied

The entrance of proton exchange membrane (PEM) fuel cells into the mass production market (e.g. in electronic devices and vehicles) is dependent upon the engineering and development of new materials (membranes and catalysts) that demonstrate improved performance characteristics accompanied by acceptable manufacturing costs. Important requirements of the proton exchange membrane include: high proton conductivity ($> 10^{-2}$ S·cm^{-1} at working temperatures > 100°C and

under low humidity conditions), suppressed solvent (H_2O) and reactant transport, and good mechanical and chemical stability. The design of new PEM materials possessing improved performance characteristics (along with decreased manufacturing costs) will require an understanding of how membrane morphology and chemical composition affect the transport of both protons and water through the material. In order to develop a coherent theoretical modeling strategy, it is necessary to bridge time and length scales, connecting the conformational equilibrium of a membrane and its general composition to molecular processes including: proton dissociation, transfer, and diffusion and hydrogen bonding, distribution, and diffusion of water.

The goals of this work were: (1) to develop a multi-scale modeling approach for studying PEMs; and (2) to elucidate microscopic proton transport mechanisms, including the roles of membrane morphology/chemical composition and relative importance of structural vs. vehicular diffusion, that will aid in the design of novel PEM materials. Our novel approach utilized both empirical and coarse-grained descriptions of the membrane to garner information useful for "informing" more accurate descriptions about large-scale characteristics such as morphology and conformational equilibria, and implemented more accurate treatments to refine the parameters of the empirical and coarse-grained approaches.

(5) Summary of the most important results

As the work involved 3 separate thrusts the important results for each thrust is described separately.

(1) DPD simulations of hydrated morphology of PFSA membranes

We undertook DPD simulations to investigate the effect of side chain chemistry of the ionomer on the hydrated morphologies of PFSA membranes including the SSC and Nafion over a range of EW's and at different water contents corresponding to intermediate levels of hydration. The PFSA polymer molecules were modeled by chains connected soft spherical particles, which represent groups of several atoms. Water was modeled as a collection of six water molecules. After geometry optimization of the particles, their corresponding Flory-Huggins χ-parameters were calculated. Based on these parameters, the DPD interaction parameters were derived and used in mesoscopic simulations to determine the morphologies of the PFSA membranes. The radial distribution functions (RDFs) of water particles have been generated and used to characterize the average sizes of water clusters. The scattering intensities were also simulated according to the Fourier transform of the RDF, and ultimately compared with recent SAXS experiments.

The equilibrated morphology of the SSC PFSA membrane of an EW = 678 is compared to Nafion with an EW = 1244 at a hydration level where $\lambda = 9$ in Figure 1 (a) and (b), respectively.

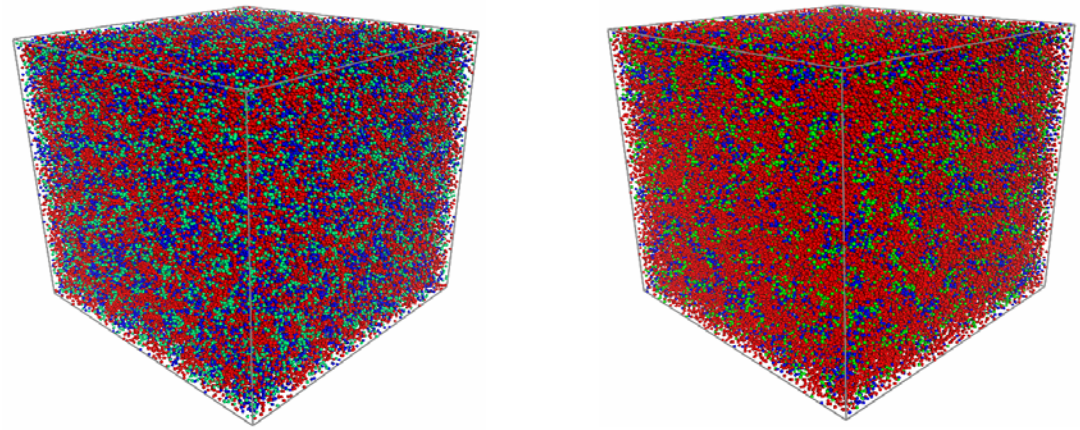

(a) (b)

Figure 1. Morphologies of the SSC and Nafion PFSA membranes at a hydration level where $\lambda = 9$: (a) SSC with an EW = 678; and (b) Nafion with an EW = 1244. The backbone beads are shown in red, the terminal portion of side chain *C* bead in green; and the water, *W*, bead in blue.

The greater connectivity to the water domains was observed at this hydration level but increasingly so at $\lambda = 16$, shown in Figure 2.

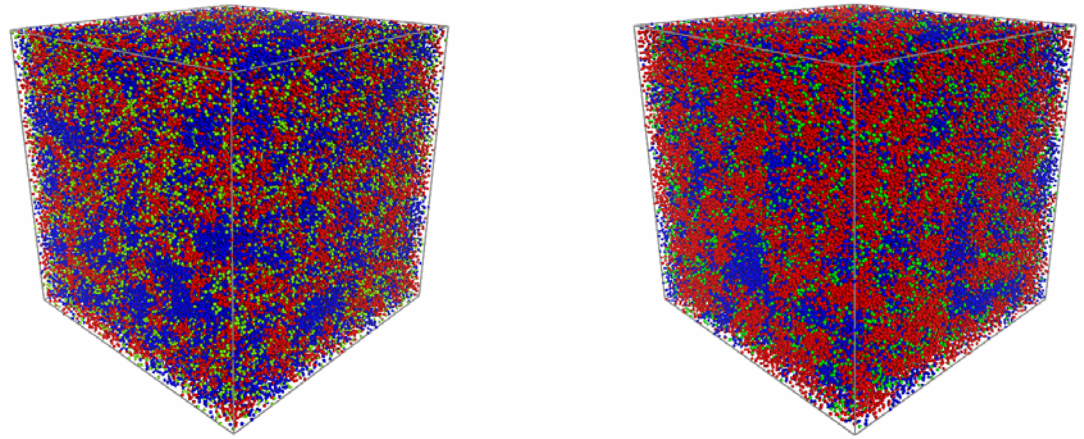

(a) (b)

Figure 2. Morphologies of the SSC and Nafion PFSA membranes at a hydration level where $\lambda = 16$: (a) SSC with an EW = 678; and (b) Nafion with an EW = 1244. The backbone beads are shown in red, the terminal portion of side chain *C* bead in green; and the water, *W*, bead in blue.

Further quantification of the differences in the morphologies of these two distinct PFSA membranes was clarified through the calculation of radial distribution functions of the water particles and are collected in Figure 3.

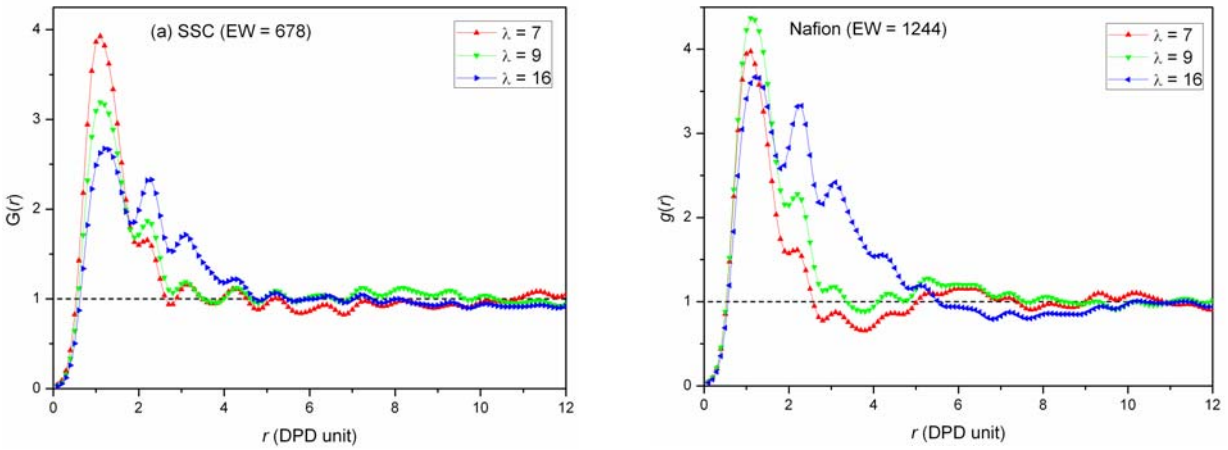

(a) (b)

Figure 3. Radial distribution functions, G(*r*)'s, of water particles at three distinct water contents: (a) SSC with an EW = 678; and (b) Nafion with an EW = 1244. The water domains at the lowest hydration level are isolated in both ionomers but the presence of the long tail at $\lambda = 16$ in the SSC system attests to the greater connectivity.

(2) Classical MD simulations of the hydration and hydronium ion diffusion of the SSC PFSA membrane

An explanation for the superior proton conductivity of low EW SSC PFSA membranes was pursued through the determination of hydrated morphology and hydronium ion diffusion

coefficients using all atom classical molecular dynamics (MD) simulations. A unique force field set for the SSC ionomer was constructed from torsion profiles determined from *ab initio* electronic structure calculations of an oligomeric fragment consisting of two side chains. MD simulations were performed on a system consisting of a single macromolecule of the ionomer (EW = 580) with the general formula F_3C-[$CF(OCF_2CF_2SO_3H)$-$(CF_2)_7$]$_{40}$-CF_3 at hydration levels corresponding to λ = 3, 6 and 13 water. Examination of the hydrated morphology indicates the formation of hydrogen bond 'bridges' between distant sulfonate groups without significant bending of the polytetrafluoroethylene backbone. Pair correlation functions of the system identified the presence of ion cages consisting of hydronium ions hydrogen bonded to three sulfonate groups at the lower water content and is shown in Figure 4. Such structures exhibit

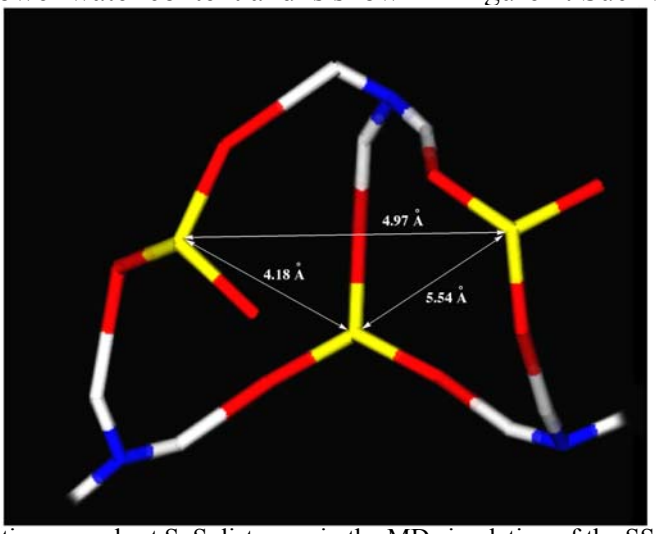

Figure 4. An ion cage exhibiting very short S–S distances in the MD simulation of the SSC ionomer. The rest of the side chain atoms in the polymer have been omitted for clarity. The two lower hydronium ions are also fully coordinated with three sulfonate groups (only two are shown).

very low S−OH_3^+ separations, well below 4 Å and severely inhibit vehicular diffusion of the protons. The number of sulfonate groups in the first solvation shell of a given hydronium ion correlates well with the differences between Nafion® and the SSC polymer (Hyflon®). The calculated hydronium ion diffusion coefficients of 2.84×10^{-7}, 1.36×10^{-6}, and 3.47×10^{-6} cm^2/s for water contents of 3, 6, and 13, respectively, show only good agreement to experimentally measured values at the lowest water content, underscoring the increasing contribution of proton shuttling or hopping at the higher hydration levels. At the highest water content the vehicular diffusion accounts for only about 1/5 of the total proton transport similar to that observed in Nafion.

(3) Car-Parrinello MD simulations of model PFSA systems

We used first principles density functional theory Car-Parrinello molecular dynamics, as implemented within CPMD, to study proton defect structures in both the native and defective crystals of: mono-, di-, and tetra- hydrates of trifluoromethanesulfonic acid to study the effects of SO_3^- interactions on proton transport as a function of water (λ= 1, 2, and 4 water/SO_3H, respectively). The generalized gradient approximation BLYP exchange correlation functional, Trouiller-Martins norm conserving pseudopotentials with an additional dispersion-corrected atom-centered potential on H, O, C, and F, a kinetic energy plane wave cut-off of 180 Ryd, the Γ-point approximation for k-point sampling, a fictitious cp mass of 300 a.u., D instead of H, and a time step of 0.05 fs were used. Kinetic energy convergence tests indicate that the energy between two configurations is reliable to ~1 kcal/mol. Monoclinic (space group $P2_1/c$) lattice

constants and positions were taken from experiment, and extrapolated to 15 K below the melting temperature if the thermal expansion coefficients were available, resulting in the following parameters: monohydrate at 293K ($H_3O^+CF_3SO_3^-$, a=5.9606 Å, b=9.9722 Å, c=9.7043 Å, β=98.685º), dihydrate at 252 K ($H_5O_2^+CF_3SO_3^-$, a=10.1532 Å, b=8.8704 Å, c=7.812 Å, β=97.646º) and tetrahydrate at 210K ($H_9O_4^+CF_3SO_3^-$, a=7.6200 Å, b=8.6804 Å, c=12.8297 Å, β=91.940º). For a given initial configuration, the positions were optimized, the temperature annealed from 0 K to the target temperature, the system equilibrated in the NVT ensemble for 10 ps using Nosé-Hoover chain thermostats on each ionic degree of freedom, and the structural data collected for at least 10 ps under the NVE ensemble. The native crystal trajectories used the published positions as the initial configuration, while the defective crystal trajectories moved one of the H^+ to a new position in a configuration taken from the native NVE trajectory.

The native crystals (see Figure 5) were found to remain almost exclusively in their native proton defect configurations: hydronium, Zundel, and Eigen cations for the mono-, di-, and tetra-hydrates, respectively. Occasionally, a proton would briefly hop to an adjacent SO_3^- or H_2O, consistent with the presolvation idea that the proton accepting species already has the proper number of H-bonds as the new proton defect structure prefers. These behaviors are indicative of either the drive for protons to be fully hydrated or the inability of nearby species to stabilize the

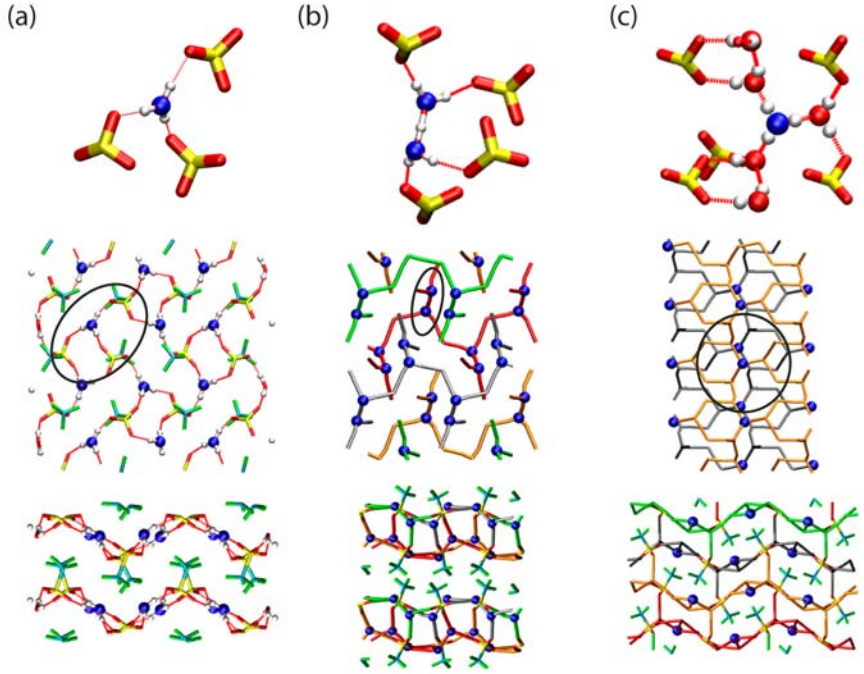

Figure 5: Snapshots of the (a) $H_3O^+CF_3SO_3^-$, (b) $H_5O_2^+CF_3SO_3^-$, and (c) $H_9O_4^+CF_3SO_3^-$ systems. Features are identified by the following scheme: H (white spheres), O (red rods), C (aqua rods), F (green rods), S (yellow rods), hydronium ions (blue spheres), and H-bonds (thin red lines). In the middle and bottom rows of (b) and (c), the green, grey, orange, and red lines connect all the H and O involved in continuous H-bonding networks. Two unit cells are shown in each direction. The top row displays the characteristic proton configuration for each crystal: hydronium, Zundel, and Eigen cations, respectively. CF_3 groups are omitted for clarity. The middle row places the proton defect, circumscribed by an ellipse, within the crystal. The bottom row highlights the H-bonding networks, revealing that the mono- and di-hydrates exhibit water layers separated by CF_3 groups, while the tetra-hydrate has connected water layers with interdigitated CF_3 groups.

new proton defect structures. The defective monohydrate crystal (see Figure 6) has an undissociated H^+ shared between *two* SO_3^- units and a Zundel cation that is stable for more than 11.9 ps. The defect motif that Eikerling *et al.* found previously is identical, although the specific

location and crystal reorganization differ substantially. These may be two examples in a large class of similar defects. The defective dihydrate crystal (see Figure 7) has an undissociated H^+ near only *one* SO_3^- unit and an Eigen-type cation that is stable ~ 13.4 ps. The defective tetrahydrate crystal (see Figure 8) rarely exhibits an undissociated H^+. Grotthuss-type proton hopping events, where a proton moves between two adjacent Eigen cations via a Zundel cation intermediate, occur frequently and often create Eigen-type cations with more water in the first solvation shell than the original Eigen-type cation.

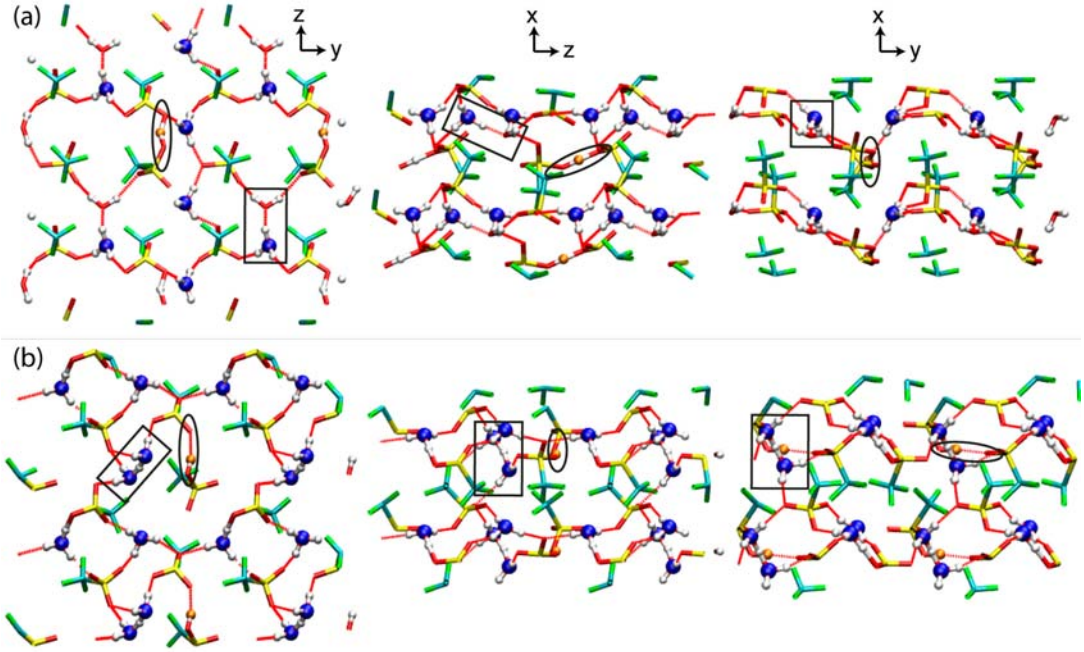

Figure 6. Snapshot of proton defects in the $H_3O^+CF_3SO_3^-$ system found in (a) this study and (b) by Eikerling *et al*.. Features are identified by the following scheme: H (white spheres), O (red rods), C (aqua rods), F (green rods), S (yellow rods), hydronium ions (blue spheres), shared undissociated H (orange), and H-bonds (thin red lines). Two unit cells are shown in each direction. The ellipses and rectangles highlight the undissociated H and Zundel cation, respectively. Both meta-stable defects have one H^+ shared between *two* SO_3 units and one Zundel cation, but the spatial location and reorganization of the crystal differs significantly.

At least on the 10-20 ps timescale, all proton transport involves Grotthuss-type proton hopping, not H_3O^+ vehicular flow. Protons did become trapped at SO_3^- units at the lowest water concentrations. At higher H_2O/ SO_3^- ratios two things happen: the protons jump more frequently into water rich local environments and the SO_3^- units become less involved in proton hopping events.

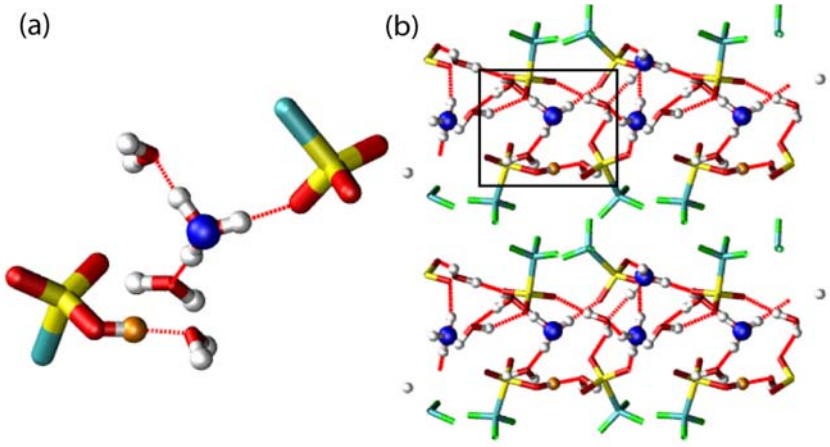

Figure 7. (a) Close-up of a proton defect and its (b) location, highlighted by the box, within the defective $H_5O_2^+CF_3SO_3^-$ crystal. Features are identified by the following scheme: H (white spheres), O (red rods), C (aqua rods), F (green rods), S (yellow rods), hydronium ions (blue spheres), undissociated H (orange), and H-bonds (thin red lines). Two unit cells are shown in each direction. Unlike the $H_3O^+CF_3SO_3^-$ crystal, the undissociated H is near only *one* SO_3^- unit and the new H^+ defect is an Eigen-type cation, with one SO_3^- nearest neighbor. The proton dissociates after ~13.4 ps.

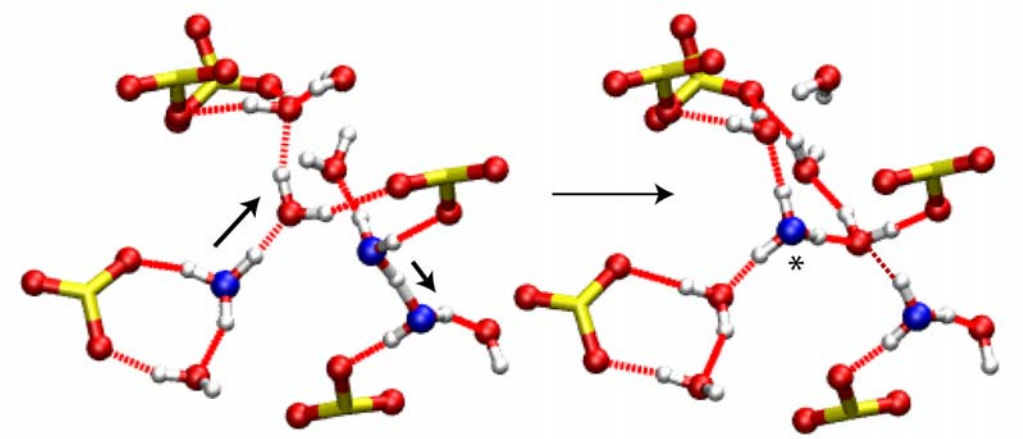

Figure 8. Snapshot of a Grotthuss-type proton transfer event in $H_9O_4^+CF_3SO_3^-$. Features are identified by the following scheme: H (white spheres), O (red rods), S (yellow rods), hydronium ions (blue spheres), and H-bonds (thin red lines). C and F are not shown for clarity. All H^+ defects are short-lived and rarely involve an undissociated H^+. Proton hops tend to create Eigen-type cations with the largest number of H_2O as nearest neighbors (see *), suggesting that protons prefer to be surround by water rather than SO_3^-.

(6) Listing of all publications and technical reports supported under this grant or contract

(a) Papers published in peer-reviewed journals

I. R. Hristov, S. J. Paddison*, and R. Paul. Molecular Dynamics Simulations of Proton Diffusion in the Short-Side-Chain Perfluorosulfonic Acid Ionomer. *ECS Transactions*, **11**, 789-796 (2007).

I. R. Hristov, S.J. Paddison*, and R. Paul Molecular Modeling of Proton Transport in the Short-Side-Chain Perfluorosulfonic Acid Ionomer. *Journal of Physical Chemistry B* **128**, 2937-2949 (2008).

(b) Papers published in non-peer-reviewed journals or in conference proceedings

None

(c) Papers presented at meetings, but not published in conference proceedings

"The Proton Exchange Membrane: Mesoscale and Molecular Modeling", invited talk, Workshop of the Israel Science Foundation: "*Diffusion, Solvation and Transport of Protons in Complex and Biological Systems*" Eilat, Israel January 13th -17th, 2008.

"Modeling Water and Transport in Hydrated Ionomers", invited lecturer, CARISMA School on: *Proton Conductors: Materials & Mechanisms,* Max-Planck-Institut für Festkörperforschung, Stuttgart, Germany November 8th – 10th, 2007.

"*Ab initio* Modeling of Structure, Reactivity, and Transfer at Water/Ionomer and Water/Catalyst Interfaces", invited talk, *Interfacial Electrochemistry and Chemistry in High Temperature*

Media, 212th National Meeting of The Electrochemical Society, Hilton Washington, Washington D.C. October 7th –12th, 2007.

"Molecular Dynamics Simulations of Proton and Water Diffusion in the Short-Side-Chain Perfluorosulfonic Acid Ionomer", contributed talk, *Proton Conducting Membrane Fuel Cells VII*, 212th National Meeting of The Electrochemical Society, Hilton Washington, Washington D.C. October 7th –12th, 2007.

"Proton Transfer in Anhydrous Polymeric Membranes for Fuel Cells: an *ab initio* study", invited speaker, symposium on "Proton Conduction and Transfer", *58th Annual Meeting of the International Society of Electrochemistry*, Banff, Canada September 9th – 14th, 2007.

"Molecular-level Modeling of Polymer Electrolyte Membranes", invited speaker, symposium on "Computational Electrochemistry for New Energy", *234th National Meeting of the American Chemical Society*, Boston, MA August 19th – 23rd, 2007.

"Molecular modeling of Proton Diffusion in the Short-Side-Chain Perfluorosulfonic Acid Ionomer", contributed talk, *Electrochemical Energy Storage and Conversion*, 90th Canadian Chemistry Conference, Winnipeg, CA May 26th–30th, 2007.

(d) Manuscripts submitted, but not published

None during the period, 2 in the period immediately following.

(e) Technical reports submitted to ARO

ARO Interim Report, 08/31/07

"Multi-scale modeling of proton transport, water distribution, and methanol permeability in Proton Exchange Membranes (PEMs)", *Progress in Advanced Energy Conversion*, The University of North Carolina at Chapel Hill, William and Ida Friday Center for Continuing Education, Chapel Hill, North Carolina September 6-7, 2007

(7) List of all participating scientific personnel showing any advanced degrees earned by them while employed on the project

Prof. Stephen J. Paddison, PI
Prof. Mark E. Tuckerman, co-PI
Dr. Dongsheng Wu, Postdoctoral researcher
Dr. Robin Hayes, Postdoctoral researcher
Mr. Iordan Hristov, Ph.D. student

(8) Report of Inventions (by title only)

None

(9) Bibliography

None to append.